Off-lattice Monte Carlo simulation of polymer brushes in good solvents

Mohamed Laradji, Hong Guo, and Martin J. Zuckermann
Centre for the Physics of Materials and Department of Physics, McGill University, Rutherford Building, 3600, rue University, Montréal, Québec, Canada H3A 2T8
(Received 5 August 1993)

We report an off-lattice Monte Carlo calculation of the equilibrium properties of a monodisperse polymer brush in a good solvent. We find that the density profile, in general, is in agreement with the results of self-consistent field theory, with some discrepancies observed near the wall and at the tail of the profile. Other quantities, such as the probability distribution of monomers, the average bond orientation, and the relative mean square displacement of monomers, are also compared with the results of the self-consistent field theory.

PACS number(s): 36.20.−r, 81.60.Jw, 82.65.Dp, 82.70.−y

I. INTRODUCTION

Considerable research effort has recently gone into the study of the structure and the physical properties of systems of uncharged polymers embedded in a solvent and end-grafted onto a solid surface. These systems are known as polymer brushes for sufficiently high polymer densities and they have wide industrial applications as adhesives, colloidal stabilizers, and lubricants [1]. For example, colloidal particles which are coated by polymer films repel each other due to the repulsive interaction between monomers, thereby inhibiting undesirable flocculation processes. The properties of the brush depends on the density of the polymers, the quality of the solvent, and the type of grafted polymer molecule among others. In this work we concentrate on uniform unbranched polymer strands in a good solvent.

Specifically, we consider an ensemble of polymer chains of length N grafted onto a substrate with a surface density σ. We also assume that the chains do not interpenetrate and that each one is uniformly distributed in a hypothetical cylinder. This cylinder has a surface area proportional to σ^{-1} and a height h. Therefore the average density of monomers is given by $\langle\phi\rangle \sim N\sigma/h$. In a good solvent the monomer-monomer interaction is dominated by excluded volume effects given by $F_{ex}/k_BT \sim w_2N^2\sigma/h$, where w_2 is the excluded volume parameter. This interaction tends to swell the polymer. The excluded volume interaction is balanced by an elastic energy given by $F_{el}/k_BT \sim h^2/N$. The competition between the two energies leads to an expression for the optimum height given by $h \sim N(w_2\sigma)^{1/3}$ [2]. The same result can be obtained using a scaling argument in which the chain is considered as a series of connected blobs, directed perpendicularly to the grafting plane, where the diameter of a blob is proportional to $\sigma^{-1/2}$, and the polymer performs a self-avoiding random walk in each blob [3]. It is important to note that these arguments, known as the Flory argument and the scaling argument, respectively, assume that the density profile of the brush is a step function.

An analytical description of polymer brushes was obtained from self-consistent field (SCF) theory where no assumption is made about the density profile. This theory was introduced by Milner, Witten, and Cates [4] and Skvorvtsov *et al.* [5]. Here the action of each separate chain is minimized independently on the basis of mean field theory giving rise to an equation for a single chain path which can be mapped onto the classical path of a point mass in a harmonic potential. Unlike either the Flory or the scaling arguments, SCF theory predicts a monotonically and parabolically decaying density profile in the direction normal to the grafting wall for moderately high grafting densities σ. It should be noted that even though the profile predicted from this theory is different from that assumed by the Flory or the scaling theories, all three theories give the same scaling form of h with N, σ, and w_2. Recently, Yeung *et al.* [6] extended SCF theory to include lateral correlations in the random phase approximation. Further theories include the work of Carignano and Szleifer [7], who used an approach based on the probability distribution function formalism of Ben-Shaul *et al.* [8] for surfactant films.

There are several numerical simulations of polymer brushes using Monte Carlo methods to move the chains on a lattice [9–11] or using molecular dynamics (MD) on the bead-spring models [12, 13]. Although some parameter fitting must be done in order to compare with the self-consistent theory results, as in the work of Lai and Zhulina [11], the simulations have the advantage of including the full effect of fluctuations. We note that due to its mean field basis, the SCF theory does not account for fluctuations around the single chain configuration which minimizes the action. The numerical simulations obtain density profiles in good agreement with SCF theory for regions not close to the two ends of the profile. A depletion layer is observed close to the grafting wall and an exponentially decaying tail is found at large distances. These two discrepancies with the SCF theory become more apparent when the grafting density is small. The numerical calculations are so far limited to a relatively small number of chains of short length, since it is difficult to move a topologically connected object on a lattice and at the same time sample enough configurations in a

Monte Carlo simulation. It is furthermore very time consuming to solve Newton equations for a large number of monomers in a MD calculation.

Until recently, the experimental verification of the theoretical predictions was mostly limited to global information concerning the brush, such as its average height but not its profile. Recently, Auroy *et al.* analyzed a brush of grafted polysterine using small-angle neutron scattering and found that the brush has essentially a parabolic profile with an exponential tail [14]. Factor *et al.* [15] used neutron reflectivity and surface tension measurements to examine the structure of diblock copolymers adsorbed at liquid ethyl benzoate–air interfaces. This system forms a polymer brush at the air interface for a considerable range of polymer densities and the authors confirm the height scaling law predicted by the above mentioned mean field and scaling theories. For the profile, they observe a depletion layer close to the surface, a parabolic profile, and an exponential tail in agreement with predictions from the simulations.

In this paper, we report an off-lattice Monte Carlo calculation of the equilibrium properties of polymer brushes with precisely the same Hamiltonian as used in SCF theory for good solvents [4, 5]. The motivation of this study is twofold. First, we wish to make a direct comparison between our results which include fluctuations and the predictions of SCF theory. Since the same Hamiltonian is used both for our calculations and for the SCF analysis, no parameter fitting is required. Second, we wish to test this method in the context of polymer brushes. As shown below, the method does indeed generate results in overall agreement with SCF theory. Since our method is very efficient, we expect that other more difficult polymer systems such as polymer melts and diblock copolymers at an interface can be successfully simulated.

The model Hamiltonian and the numerical method used for our calculations are described in Sec. II. The numerical results are presented and compared with the SCF predictions in Sec. III. These include the density profiles for several sets of parameters, the probability distributions, the average of the bond orientation, and other results. Our results are discussed in the context of existing theoretical work in Sec. IV.

II. MODEL AND NUMERICAL METHOD

We first describe the Edwards Hamiltonian used in this paper [16]. Let $\mathbf{r}_i(n)$ be the position of the nth monomer on on the ith polymer chain. The Hamiltonian for a monodisperse polymer solution consisting of K chains, each composed of $(N+1)$ monomers is written as follows:

$$\frac{\mathcal{H}\{\mathbf{r}_i(n)\}}{k_B T} = \frac{1}{2}\sum_{i=1}^{K}\int_0^N dn\left(\frac{d\mathbf{r}_i(n)}{dn}\right)^2 + \mathcal{V}\{\mathbf{r}_i(n)\}. \tag{1}$$

The first term is the sum of Gaussian stretches of two neighboring monomers on the same chain. $\mathcal{V}\{\mathbf{r}_i(n)\}$ is a short-range interaction potential between monomers. In the case of polymers mixed with a good solvent, $\mathcal{V}$ is the second term in the virial expansion of the interaction energy and corresponds to the excluded volume interaction. In this case it is given by

$$\mathcal{V}\{\mathbf{r}_i(n)\} = \frac{1}{2} w_2 \int d\mathbf{r}\phi^2(\mathbf{r}), \tag{2}$$

where a good solvent is characterized by a positive value of w_2. $\phi(\mathbf{r})$ is the local concentration of monomers which can be written as

$$\phi(\mathbf{r}) = \sum_{i=1}^{K}\int_0^N dn\delta(\mathbf{r} - \mathbf{r}_i(n)). \tag{3}$$

The Hamiltonian can then be rewritten as follows using Eq. (3):

$$\frac{\mathcal{H}\{\mathbf{r}_i(n)\}}{k_B T} = \frac{1}{2}\sum_{i=1}^{K}\int_0^N dn\left[\left(\frac{d\mathbf{r}_i(n)}{dn}\right)^2 + w_2\phi(\mathbf{r}_i(n))\right]. \tag{4}$$

In our simulations, we used $w_2 = \frac{1}{2}$ for the second virial coefficient. The third virial coefficient is required in the case of a poor solvent or a Θ solvent. In order to calculate ϕ from the the spatial positions of the monomers, appropriate coarse graining is required. One possibility is to devide the system into a fine cubic grid and count the number of monomers in each cube. Another method is to coarse grain via a Gaussian function. We found both methods give essentially the same results. For the simulations described in this paper, we used the following Gaussian form for the coarse graining to obtain ϕ,

$$\phi(\mathbf{r}_i(n)) = \left(\frac{1}{b\sqrt{\pi}}\right)^3 \times \sum_{j=1}^{K}\int_0^N dm \exp\left(-\frac{[\mathbf{r}_i(n) - \mathbf{r}_j(m)]^2}{b^2}\right)\Bigg|_b. \tag{5}$$

Here b is small but finite and for the results reported here we have fixed $b = 0.4$. In our simulations the system configuration is described by the spatial positions of the individual monomers. Thus the integration in (5) is replaced by a summation. In our representation of the polymer brush, one end of each polymer chain is grafted at a random position on the substrate corresponding to the xy plane ($z = 0$). The other monomers are constrained to lie in the upper half-space ($z \geq 0$). The simulations are carried out using the standard Metropolis Monte Carlo technique in real space. At every Monte Carlo move, we attempt to change the position $\mathbf{r}_i(n)$ of a monomer and compute the local concentration ϕ using Eq. (5). This new value of ϕ is then substituted into the Hamiltonian (4) to calculate the energy change due to this attempted move. The move is then accepted or rejected using this energy change according to the Boltzmann probability in the usual way. Since detailed balance is always satisfied by the algorithm, the equilibrium state will be reached after a sufficient number of Monte Carlo moves. In this algorithm, the connectivity of a chain is automatically ensured by the stretching term in the Hamiltonian. Hence moving nearest neighbor monomers too far apart costs

a large amount of energy and any configurations of this type will therefore be rejected.

For all simulations, we used $K = 100$ chains with $(N + 1)$ monomers each, where $N = 40$, 60, and 100. The grafting densities used in the simulation correspond to $\sigma = \frac{K}{S} = 0.05$, 0.1, 0.16, and 0.2, where S is the area of the grafting substrate. For $N = 100$ we only considered the first three values of σ. 10^5 Monte Carlo steps per monomer were used for each simulation, including equilibration of the system. For the initial condition, we used a fully stretched profile with small fluctuations in the monomer positions.

III. RESULTS

The physical quantities calculated in our simulations were chosen to be those which were also analyzed by the SCF theory. Figures 1(a) and 1(b) show several density profiles obtained from our simulations for different surface densities and chain lengths. These profiles clearly show a depletion layer adjacent to the grafting surface. In contrast with SCF theory which does not predict such a depletion layer, almost all previous numerical simulations [9–12] and some numerical mean field calculations on finite chain brushes [7, 17, 18] show the same behavior. We discuss the scaling of the depletion layer below. As expected, the profiles have a monotonic decay instead of the constant profile predicted by the scaling and the Flory arguments [2, 3]. For distances far from the grafting plane, we observe that the density profile decays to zero smoothly in contrast to that predicted by SCF theory. This is in good agreement with the prediction of Milner [1] for finite chains, i.e.,

$$\phi(z) \sim \exp[-C(z-h)^{3/2}], \tag{6}$$

where C scales as $N^{-1/2}\sigma^{1/6}$ and h is the brush height obtained from SCF theory [4, 5]. This implies that the tail of the profile has a length scale which is given by $l_{\text{tail}} \sim N^{1/3}\sigma^{-1/9}$. Therefore, relative to the height of the brush, l_{tail}/h becomes vanishingly small as the polymer chains become infinitely long. The MD simulations of Murat and Grest [12] and the mean field calculations of Carignano and Szleifer [7] show the presence of a region at intermediate distances from the grafting plane over which the density profile is flat for grafting densities $\sigma \geq 0.1$. Our Monte Carlo simulations do not see such profiles even for grafting densities as high as $\sigma = 0.2$. The reason that the MD simulations see a flat profile may be due to the fact that the interaction potential used in these simulations contains higher order terms in the virial expansion, whereas the Hamiltonian used in our simulations does not explicitly contain high order terms. In fact, using SCF theory, it can be shown that a rather flat profile can be obtained from the full Flory-Huggins free energy [1].

The SCF theory predicts the following density profile for relatively high grafting densities and long chains:

$$\phi(z) = \frac{\pi^2}{8N^2 w_2}(h^2 - z^2)\ \theta(h - z), \tag{7}$$

where the brush height h is given by

$$h = \left(\frac{12}{\pi^2}\right)^{1/3} (\sigma w_2)^{1/3} N. \tag{8}$$

Equations (7) and (8) lead to the following scaling form for ϕ:

$$\frac{\phi(z)}{\sigma^{2/3}} = \frac{\pi^2}{8w_2}(H^2 - Z^2)\ \theta(H - Z), \tag{9}$$

where $H = h/(\sigma^{1/3}N)$ and $Z = z/(\sigma^{1/3}N)$ are the rescaled brush height and the rescaled distance from the grafting plane, respectively. In order to check the existence of such a scaling and to compare explicitly with the SCF theory, we show in Fig. 2 the scaled profile $\phi(z)/\sigma^{2/3}$ as a function of the scaled distance form the wall $z/(N\sigma^{1/3})$ for all the systems investigated by our simulations together with the SCF prediction (solid line).

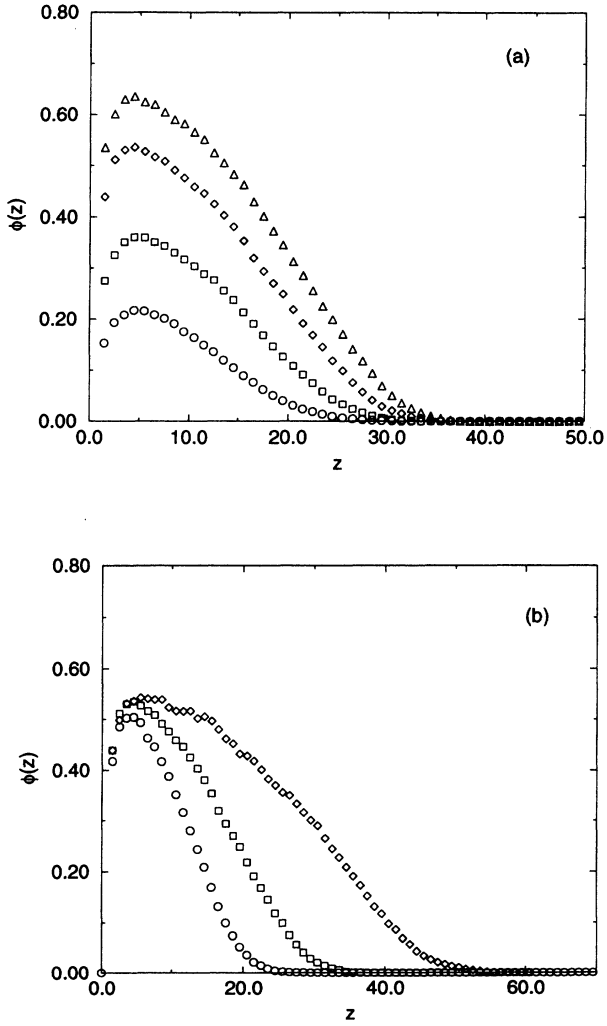

FIG. 1. Density profile $\phi(z)$ as a function of the distance from the grafting plane z. (a) corresponds to $N = 60$ and $\sigma = 0.05$ (circles), $\sigma = 0.1$ (squares), $\sigma = 0.16$ (diamonds), and $\sigma = 0.2$ (triangles), and (b) corresponds to $\sigma = 0.16$ and $N = 40$ (circles), $N = 60$ (squares), and $N = 100$ (diamonds).

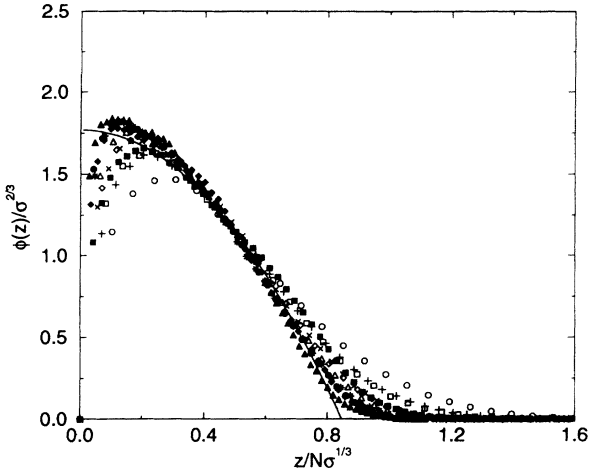

FIG. 2. Scaled density profiles $\phi(z)/\sigma^{2/3}$ as a function of scaled distance from the grafting plane $z/(N\sigma^{1/3})$ for $(N,\sigma) = (40,0.05)$ (open circles), (40,0.1) (open squares), (40, 0.16) (open diamonds), (40,0.2) (open triangles), (60,0.05) (pluses), (60,0.1) (crosses), (60,0.16) (stars), (60,0.2) (close circles), (100,0.05) (close squares), (100,0.1) (close diamonds), and (100,0.16) (close triangles). The solid line corresponds to the SCF prediction, Eq. (9).

Apart from the region close to the grafting plane and the tail of the profiles, our Monte Carlo data collapses reasonably well onto a universal curve. As expected the data collapse of the density profiles improves with increasing values of σ and N. Furthermore, the simulated density profiles collapse onto the scaled SCF density profile given by Eq. (9).

Scaling arguments predict that the size of the depletion layer scales as $\sigma^{-1/2}$ [19]. In order to check this scaling, we show $\phi(z)/\sigma^{2/3}$ as a function of $z\sigma^{1/2}$ in Fig. 3. From this figure it can be seen that all systems with different values of N and σ follow a master curve close to the grafting plane for $z\sigma^{1/2} \leq 0.7$ in agreement with the above scaling.

The scaling form predicted by the Flory argument or

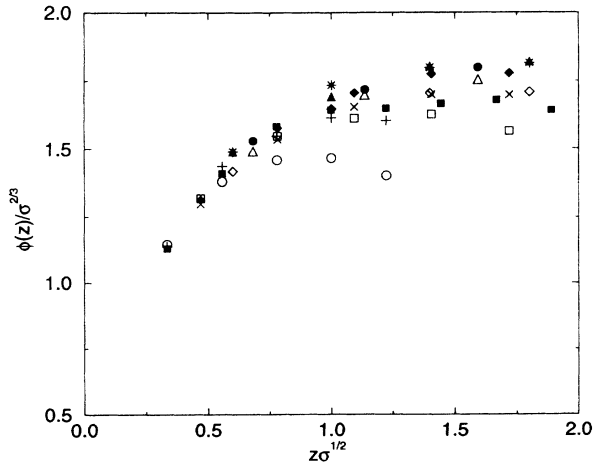

FIG. 3. The scaled density profile $\phi(z)/\sigma^{2/3}$ as a function of $z\sigma^{1/3}$.

SCF theory implies that for large N, there is only one relevant length scale along the axis normal to the grafting plane. This length scale can be considered from several points of view. In this context and in order to be consistent with previous analytical and numerical calculations, we studied the length scale by calculating the average thickness of the brush

$$\langle z\rangle = \frac{\int_0^\infty dz z\phi(z)}{\int_0^\infty dz\phi(z)} \tag{10}$$

and the square of z component of the radius of gyration

$$\langle R_{gz}^2\rangle = \frac{1}{K}\sum_{i=1}^{K}\left\langle \frac{1}{N}\int_0^N dn\left(z_i(n) - \frac{1}{N}\int_0^N dn z_i(n)\right)^2\right\rangle. \tag{11}$$

SCF theory predicts that the average thickness and the z component of the radius of gyration are given by

$$\langle z\rangle = \frac{3}{8}\left(\frac{12w_2\sigma}{\pi^2}\right)^{1/3} N \tag{12}$$

and

$$\langle R_{gz}^2\rangle = \frac{2}{5}\left(\frac{1}{2} - \frac{4}{\pi^2}\right)\left(\frac{12w_2\sigma}{\pi^2}\right)^{2/3} N^2, \tag{13}$$

respectively. Figure 4 gives our numerical values for the scaled brush thickness, $\langle z\rangle/(N\sigma^{1/3})$ versus $N\sigma^{1/3}$, and the scaled radius of gyration, $\langle R_{gz}^2\rangle^{1/2}/(N\sigma^{1/3})$, together with the lines predicted by Eqs. (12) and (13). A scaling behavior in the density profile is expected to hold when both of these lengths become independent of $N\sigma^{1/3}$. Although our numerical prediction shows that we are not as yet in the scaling regime, the trend of the data indicates that $\langle z\rangle$ and $\langle R_{gz}^2\rangle^{1/2}$ are converging towards the SCF

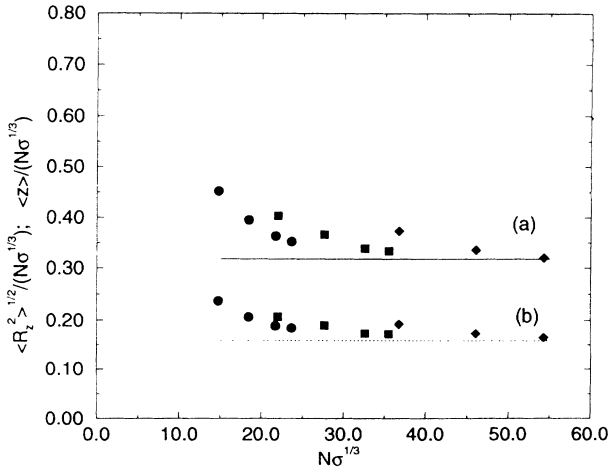

FIG. 4. (a) Average thickness $\langle z\rangle/(N\sigma^{1/3})$ and (b) the z component of the radius of gyration $\langle R_{gz}^2\rangle^{1/2}/(N\sigma^{1/3})$ as a function of $N\sigma^{1/3}$. The solid line is from Eq. (12) and the dotted line is from Eq. (13). Circles correspond to $N = 40$, squares correspond to $N = 60$, and diamonds correspond to $N = 100$.

values. We also note that for small values of N, the value of $N\sigma^{1/3}$ at which the scaling regime begins is itself small. This can be understood using simple scaling arguments. Such an argument is based on a crossover from a brush of stretched polymers where $\langle z\rangle \sim N\sigma^{1/3}$ to a brush of nonstretched polymers where the radius of gyration is smaller than the average distance between grafting sites. This is expected to occur when $N^{3/5} \sim 1/\sigma^{1/2}$, i.e., when $N\sigma^{1/3} \sim N^{3/5}$. This shows that the crossover point increases with increasing N. A similar result was obtained by Murat and Grest from their MD simulation [12].

For further comparisons with SCF theory, we calculated the probability distributions of a sequence of monomers on a chain. Figure 5 shows normalized distributions for $\sigma = 0.1$ and $N = 60$. We observe that the distribution $\rho_n(z)$ becomes more extended as the monomer index n increases and its width is greatest for the free ends of the polymers, as expected.

SCF theory predicts the following form for the probability distribution of a given monomer n,

$$\rho_n(z) = \frac{3z}{\left[h\sin\left(\frac{n\pi}{2N}\right)\right]^2}\sqrt{1-\left[\frac{z}{h\sin\left(\frac{n\pi}{2N}\right)}\right]^2} \times\theta\left[h\sin\left(\frac{n\pi}{2N}\right)-z\right]. \quad (14)$$

This implies that the distribution follows a simple scaling form, i.e., $\rho_n(z)\sin(\frac{n\pi}{2N})$ is a function of $z/\sin(\frac{n\pi}{2N})$ independent of the monomer index n. In Fig. 6 we show the scaled probability distributions for three different parameters and compare them to SCF theory. First, reasonably good scaling is observed apart from the monomers with low index n relatively close to the grafting surface. As expected, the comparison between our scaled distribution and the SCF prediction improves as both N and σ increase. The comparison is best for the region to the left of the maximum in the distribution. An important result is that all our data show distributions which are rather concave in this region in agreement with the SCF results [4, 5]. Previous lattice Monte Carlo simulations [9–11], however, obtained distributions which are convex for small $z/\sin(\frac{n\pi}{2N})$. This is believed to be due to the finite stretching of monomers in these models as has been shown by an SCF theory which takes into account this effect [20]. Finally, for larger values of z our distributions decay more slowly than the SCF prediction in agreement with other Monte Carlo [9–11] and MD simulations [12].

A further comparison with the SCF theory can be made for the average height $\langle z_n\rangle$ of the nth monomer. SCF theory predicts that

$$\langle z_n\rangle = \langle z_N\rangle \sin\frac{n\pi}{2N} = \frac{3\pi}{16}h\sin\frac{n\pi}{2N}. \quad (15)$$

Figure 7 shows the scaled average distance of the nth monomer from the grafting layer $\langle z_n\rangle/(N\sigma^{1/3})$ as a function of n/N together with the SCF prediction. This figure shows that the simulation results agree quite well with SCF theory, particularly for high values of N and σ.

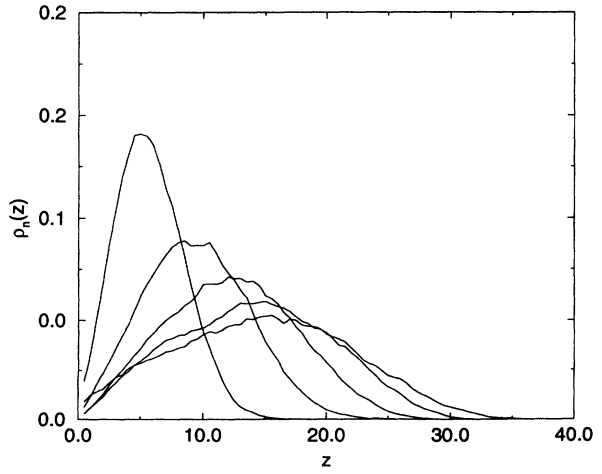

FIG. 5. The monomer probability distribution for $N = 60$ and $\sigma = 0.1$. Curves from top to bottom correspond to n/N=0.2, 0.4, 0.6, 0.8, and 1, respectively.

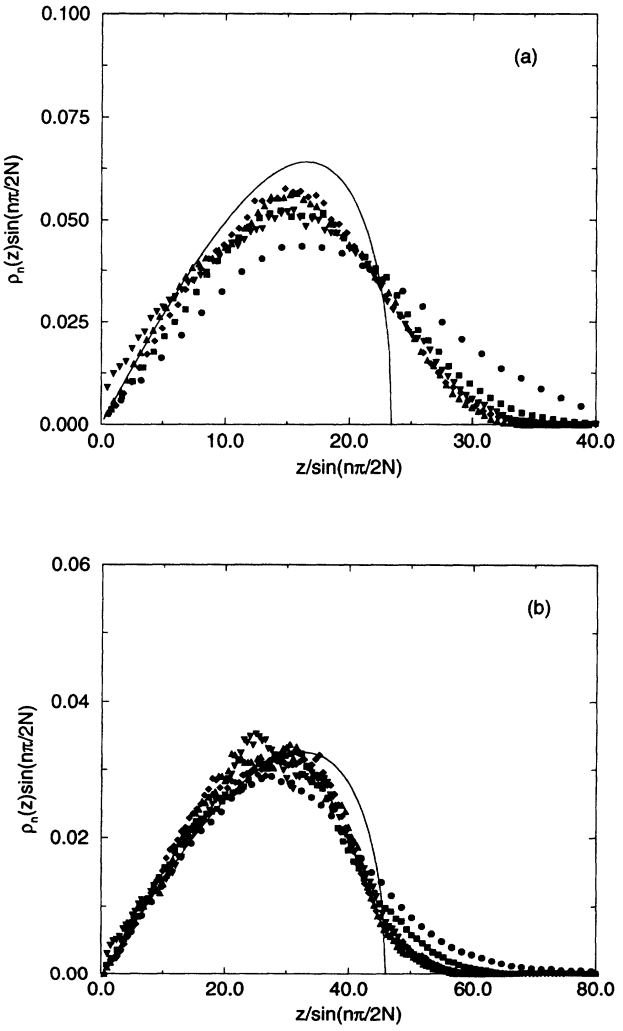

FIG. 6. The scaled distribution probability for (a) $N = 60$ and $\sigma = 0.1$ and (b) $N = 100$ and $\sigma = 0.16$. The points correspond to $n/N = 0.2$ (circles), $n/N = 0.4$ (squares), $n/N = 0.6$ (diamonds), $n/N = 0.8$ (up triangles), and $n/N = 0.8$ (down triangles).

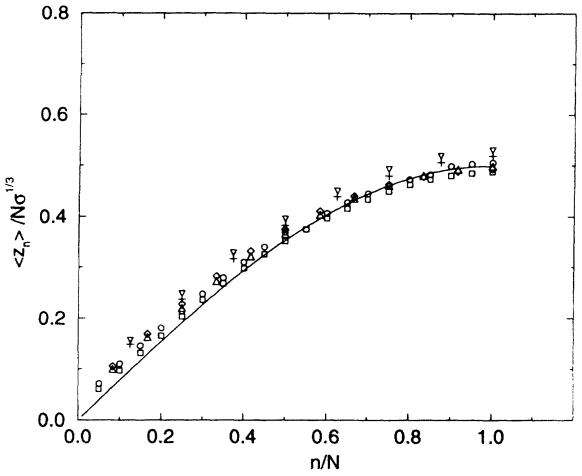

FIG. 7. Average height of monomers $\langle z_n \rangle$ as a function of n/N. The solid curve correspond to Eq. (12) normalized by $N\sigma^{1/3}$. Shown data correspond to $(N, \sigma) = (100,0.1)$ (circles), (100,0.16) (squares), (60,0.16) (diamonds), (60,0.2) (up triangles), (40,0.16) (down triangles), and (40,0.2) (pluses).

Another comparison with SCF theory can be made via the average orientation of the monomers along the chain as characterized by $\cos\theta_n$, where θ_n is the angle that the bond between the $(n-1)$th monomer and nth monomer makes with the z axis. In this case SCF theory predicts

$$\langle \cos\theta_n \rangle = \frac{1}{K}\sum_{i=1}^{K}\left\langle \frac{z_i(n) - z_i(n-1)}{|\mathbf{r}_i(n) - \mathbf{r}_i(n-1)|} \right\rangle = \frac{3}{16}\left(\frac{3}{2}\pi^4 w_2 \sigma\right)^{1/3} \cos\frac{n\pi}{2N}. \quad (16)$$

The average cosine of the bond angle has a scaling form $\langle \cos\theta_n \rangle/\sigma^{1/3}$, which is a function of n/N only. Figure 8 shows $\langle \cos\theta_n \rangle/\sigma^{1/3}$ as a function of n/N for all the systems studied to compare with the theoretical prediction. Once again, the Monte Carlo results compare reasonably well with the SCF theory results, except for the monomers close to the grafting surface. The behavior of this function close to the grafting surface is, however, similar to previous brush simulations. Figure 8 implies that the first few bonds of the chain close to the grafting surface are considerably more stretched than the other bonds in the chain. This is due to an effective repulsion with the grafting surface and should be correlated with the depletion layer shown in the density profile. Moreover, the average cosine of the bond angle is always positive which indicates that on average the polymer chains do not fold back on each other and are therefore extended. This is consistent with the behavior of the average distance $\langle z_n \rangle$ from the grafting plane which always increases as n increases.

We also calculated the relative mean square displacement of the monomer positions along the z axis $\langle \Delta z_n^2 \rangle/\langle z_n \rangle^2$. This quantity is shown in Fig. 9(a) for $\sigma = 0.05$ and several system sizes and in Fig. 9(b) for $N = 40$ and several grafting densities. Our results are shown together with the mean square displacement predicted by SCF theory,

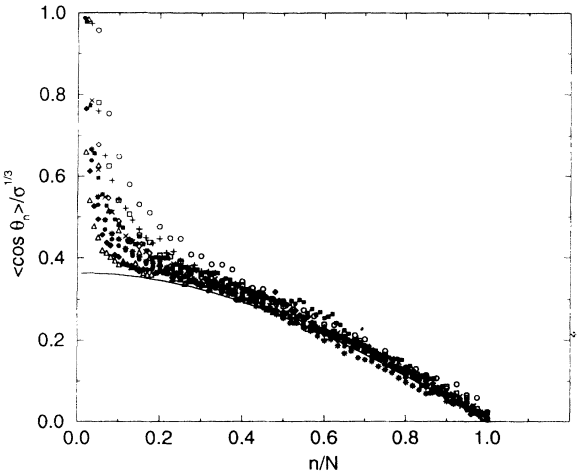

FIG. 8. Normalized cosine of monomer bonds $\langle \cos\theta_n \rangle/\sigma^{1/3}$ versus n/N for $(N, \sigma) = (40,0.05)$ (open circles), (40,0.1) (open squares), (40, 0.16) (open diamonds), (40,0.2) (open triangles), (60,0.05) (pluses), (60,0.1) (crosses), (60,0.16) (stars), (60,0.2) (close circles), (100,0.05) (close squares), (100,0.1) (close diamonds), and (100,0.16) (close triangles). The solid line is the SCF prediction from Eq. (16).

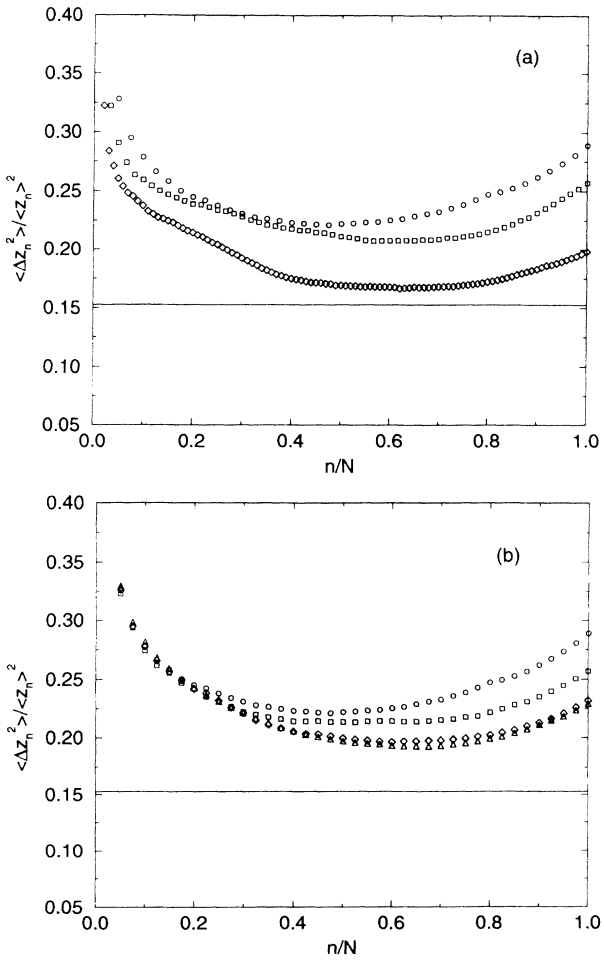

FIG. 9. Mean square displacement of monomers for (a) $\sigma = 0.05$ and $N = 40$ (circles), $N = 60$ (squares), and $N = 100$ (diamonds), and (b) $N = 40$ and $\sigma = 0.05$ (circles), $\sigma = 0.1$ (squares), $\sigma = 0.16$ (diamonds), and $N = 0.2$ (triangles).

$$\frac{\langle \Delta z_n^2 \rangle}{\langle z_n \rangle^2} = \frac{2}{5}\left(\frac{16}{3\pi}\right)^2 - 1 = 0.1528. \quad (17)$$

This is a constant which is independent of grafting density N and monomer index n. Figure 9 shows that our results are quite different from the SCF predictions, as was the case with the results of lattice Monte Carlo simulations [10, 11]. Instead of a constant, the data show a minimum which approaches the SCF value, Eq. (17), as N or σ are increased. Furthermore, there is a flat region around the minimum which becomes broader with increasing N. Finally, our calculated values for $\langle \Delta z_n^2 \rangle / \langle z_n \rangle^2$ are always larger than those predicted by SCF theory, since the distributions obtained from our simulations are broader than the SCF distributions. Our results are in contrast to those previously found from lattice Monte Carlo simulations [10, 11] which give smaller values for $\langle \Delta z_n^2 \rangle / \langle z_n \rangle^2$ than those found from SCF theory. The fact that they obtained smaller values is due to the finite extensibility of monomers in their models which results in probability distributions narrower than those predicted from SCF theory [4, 5]. This has been shown by the work of Shim and Cates [20].

IV. DISCUSSION

In summary, we have studied the equilibrium properties of a polymer brush in a good solvent using a direct Metropolis Monte Carlo method for the Edwards Hamiltonian. The computational advantage of this algorithm is the absence of the topological constraints enforced in many standard numerical methods. Our results are in good agreement with those of SCF theory with some differences which can be ascribed to the presence of fluctuations in the simulations resulting from finite chains. In particular, we found that physical quantities such as the density profile, the average monomer height, and the average bond cosine of the brush compare well with the results of SCF theory [4, 5].

For the monomer position probability distribution $\rho_n(z)$ we observed reasonable scaling between the distributions of different monomers as expected from SCF theory, but the shape of the scaling function was somewhat different from the SCF result. That the numerical distributions are always broader than the SCF prediction can be understood since fluctuations present in the simulations always try to make the monomer position more uncertain. The comparison between our simulation results and the SCF predictions improves as N and σ increase. Thus it is likely that in the large N and σ limit, the Monte Carlo simulation will approach the SCF results completely. For finite N and small values of σ as studied here, the distributions which are broader than the SCF prediction lead to larger values of the relative mean square displacement of monomers along the z axis than the SCF prediction. The SCF theory [4, 11] predicts a relative mean square displacement which is independent of σ, N, and particularly the monomer index n. In our simulations, we observed that the relative mean square displacement depends on the monomer index n. This is because the probability distributions for different monomers have not reached scaling regime completely.

We note that the differences between our Monte Carlo results and those of SCF theory are similar to what was found by Lai and Zhulina [11] where they used the bond-fluctuation algorithm to move the polymer chains on a lattice. They proposed that the differences which they observed could be caused by deviations from Gaussian stretching. Differences may also occur since the bond-fluctuation model contains higher order terms in the virial expansion while SCF theory for good solvents used only the second virial coefficient. In our simulations we used the same Hamiltonian as that of SCF theory but obtained similar results as those from the bond-fluctuation algorithm. It is therefore likely that the difference between Monte Carlo simulations and SCF theory are due to fluctuations which decrease with increasing N and σ.

The presence of both a depletion layer and an exponentially decaying tail in the density profile have been observed in previous numerical SCF [17, 18], in Monte Carlo simulations [9–11] and in molecular dynamics simulations [12]. We have also observed such a behavior in our simulations. While the depletion layer is due to an effective repulsion between the monomers and the grafting wall, the presence of a decaying tail is closely related to the shape of the monomer distribution function, as shown in Fig. 6. The monomer distribution function, when computed using SCF theory, has a sharp cutoff to zero. However, our Monte Carlo simulations give a slow decay at large z values due to fluctuations in the monomer positions at the end of the brush. The difference in the distribution functions gives rise to the difference in the tail region of the brush density profiles. Apart from these differences our data agree well with the SCF prediction of the density profile. Given the general agreement with SCF theory, we conclude that fluctuations do not strongly affect the physical properties of polymer brushes in a good solvent in the framework of the Edwards model. However, fluctuation effects may be considerably more important for the case of poor solvents.

The applications of the direct Monte Carlo method presented in this paper are not restricted to the verification of the results of SCF theory. This method enables us to study more difficult situations where analytical theory has limited predictive power. For instance, we can study the effects of thermal fluctuations which were not understood previously. We are at present applying this method to the study of polymer brushes in a poor solvent for which recent simulations using the bond–fluctuating model [11], molecular dynamics method [21], and calculations based on the random phase approximation [6] indicate the occurrence of microphase separation. Finally, we point out that while the direct Monte Carlo method as applied here allows the system to go to equilibrium, the dynamics used to relax the system does not reflect reality. In order to study the dynamics one must employ more appropriate techniques.

ACKNOWLEDGMENTS

We thank Professor R. Dickman, Professor K. Zhulina, Professor P. Y. Lai, Professor D. Jasnow, and Dr. C. Yueng for many useful discussions and generous help. H.G. has benefited from conversations with Professor G. Slater. This work is supported by the Natural Sciences and Engineering Research Council of Canada and Le Fonds pour la Formation des Chercheurs et l'Aide à la Recherche de la Province de Québec via both a center and a team grant.

[1] S. T. Milner, Science **251**, 905 (1991).
[2] S. Alexander, J. Phys. (Paris) **38**, 983 (1977).
[3] P. G. de Gennes, Adv. Colloid Interface Sci. **27**, 189 (1987).
[4] S. T. Milner, T. A. Witten, and M. E. Cates, Marcromolecules **21**, 2610 (1988).
[5] A. M. Skvortsov, A. A. Gorbunov, I. V. Pavlushkov, E. B. Zhulina, O. V. Borisov, and V. A. Priamitsyn, Polym. Sci. USSR **30**, 1706 (1988).
[6] C. Yeung, A. C. Balasz, and D. Jasnow, Macromolecules **26**, 1914 (1993).
[7] M. A. Carignano and I. Szleifer, J. Chem. Phys. (to be published).
[8] A. Ben-Shaul, I. Scleifer, and W. M. Gelbart, J. Chem. Phys. **83**, 3597 (1985).
[9] A. Chakrabarti and R. Toral, Macromolecules **23**, 2016 (1990).
[10] P.-K. Lai and K. Binder, J. Chem. Phys. **95**, 9288 (1991).
[11] P.-K. Lai and E. B. Zhulina, J. Phys. II (Paris) **2**, 547 (1992).
[12] M. Mural and G. S. Grest, Macromolecules **22**, 4054 (1989).
[13] M. Murat and G. S. Grest, Phys. Rev. Lett. **63**, 1074 (1989).
[14] P. Auroy, Y. Mir, and L. Auvray, Phys. Rev. Lett. **69**, 93 (1992).
[15] B. J. Factor, L.-T. Lee, M. S. Kent, and F. Rondelez (unpublished).
[16] M. Doy and S. F. Edwards, *The Theory of Polymer Dynamics* (Oxford University Press, London, 1986), pp. 25 and 26.
[17] J. M. H. M. Scheutjens and G. J. Fleer, J. Phys. Chem. **83**, 1619 (1979); G. J. Fleer, Colloids Surf. **35**, 151 (1989).
[18] T. Cosgrove, T. Heath, B. Van Lent, F. Lerrmakers, and J. Scheutjens, Macromolecules **20**, 1692 (1987).
[19] P. G. de Gennes, Macromolecules **13**, 1069 (1980).
[20] D. F. K. Shim and M. E. Cates, J. Phys. (Paris) **50**, 3535 (1989).
[21] G. S. Grest and M. Murat, Macromolecules **26**, 3108 (1993).